Proceedings of the ASME 2013 7th International Conference on Energy Sustainability & 11th Fuel Cell Science, Engineering and Technology Conference
ESFuelCell2013
July 14-19, 2013, Minneapolis, MN, USA

ES-FuelCell2013-18186

OPTICAL ANALYSIS OF A WINDOW FOR SOLAR RECEIVERS USING THE MONTE CARLO RAY TRACE METHOD

Ahmet Murat Mecit
Combustion and Solar Energy Laboratory,
Department of Mechanical Engineering
San Diego State University
San Diego, CA, USA
ahmetmuratmecit@gmail.com

Fletcher Miller
Combustion and Solar Energy Laboratory,
Department of Mechanical Engineering
San Diego State University,
San Diego, CA, USA
Fletcher.Miller@sdsu.edu

ABSTRACT

Concentrated solar power (CSP) systems use heliostats to concentrate solar radiation in order to produce heat, which drives a turbine to generate electricity. We, the Combustion and Solar Energy Laboratory at San Diego State University, are developing a new type of receiver for power tower CSP plants based on volumetric absorption by a gas-particle suspension. The radiation enters the pressurized receiver through a window, which must sustain the thermal loads from the concentrated solar flux and infrared reradiation from inside the receiver. The window is curved in a dome shape to withstand the pressure within the receiver and help minimize the stresses caused by thermal loading. It is highly important to estimate how much radiation goes through the window into the receiver and the spatial and directional distribution of the radiation. These factors play an important role in the efficiency of the receiver as well as window survivability.

Concentrated solar flux was calculated with a computer code called MIRVAL from Sandia National Laboratory which uses the Monte Carlo Ray Trace (MCRT) method. The computer code is capable of taking the day of the year and time of day into account, which causes a variation in the flux. Knowing the concentrated solar flux, it is possible to calculate the solar radiation through the window and the thermal loading on the window from the short wavelength solar radiation. The MIRVAL code as originally written did not account for spectral variations, but we have added that capability.

Optical properties of the window such as the transmissivity, absorptivity, and reflectivity need to be known in order to trace the rays at the window. A separate computer code was developed to calculate the optical properties depending on the incident angle and the wavelength of the incident radiation by using data for the absorptive index and index of refraction for the window (quartz) from other studies and vendor information. This method accounts for regions where the window is partially transparent and internal absorption can occur.

A third code was developed using the MCRT method and coupled with both codes mentioned above to calculate the thermal load on the window and the solar radiation that enters the receiver. Thermal load was calculated from energy absorbed at various points throughout the window. In our study, window shapes from flat to concave hemispherical, as well as a novel concave ellipsoidal window are considered, including the effect of day of the year and time of the day.

INTRODUCTION

Concentrated solar power (CSP) systems use mirrors to concentrate the solar radiation. The concentrated solar radiation is used to heat a working fluid which drives a turbine to generate electricity. There are four types of CSP technologies: parabolic troughs, dish/engine systems, Linear Fresnel reflectors and power towers, shown in Figure 1 [1]. These systems can be categorized depending on the focus type, as line focus collectors and point focus collectors. Linear Fresnel Reflectors (LFRs) and the parabolic troughs have line focus collectors which mean that the collectors are lined in a single axis in order to make tracking the sun simpler. On the other hand, the dish/engine systems and the power towers have point focus collectors which means that the collectors track the solar radiation along two axes to focus the solar radiation to a single point in order to achieve higher temperatures [2].

 Copyright © 2013 by ASME

Power towers use a field of heliostats to concentrate the solar radiation to the focal point of the heliostats. The heliostat is a computer-controlled device that consists of mirrors and moves throughout the day in order to concentrate the solar radiation to a designated target, called the aim point. A receiver is located at the designated target on a tower called a power tower. The fluid flowing inside the receiver is heated by the concentrated radiation, with the details depending on the receiver design. The heat drives a thermodynamic cycle, generally a Rankine cycle on commercial plants, to generate electricity. Compared to the LFRs and parabolic troughs, power towers can reach higher temperatures. The reason is that more solar radiation is concentrated on a smaller surface area which will reduce the heat losses. The thermodynamic cycles are more efficient when operating at higher temperatures. Therefore, higher efficiency can be achieved with power tower systems. These potential advantages make the power tower systems more appealing. These systems could soon become the preferred CSP technology [3]. One of the challenges with central receivers, however, is the receiver design. Current commercial receivers cannot sustain the highest fluxes that a heliostat field is capable of producing, especially if using a gas as the working fluid, which is the desired working fluid for a gas turbine offering higher efficiency than the Rankine systems in use today. Therefore, we have initiated research on an older concept for a gas-cooled receiver as described in the next section.

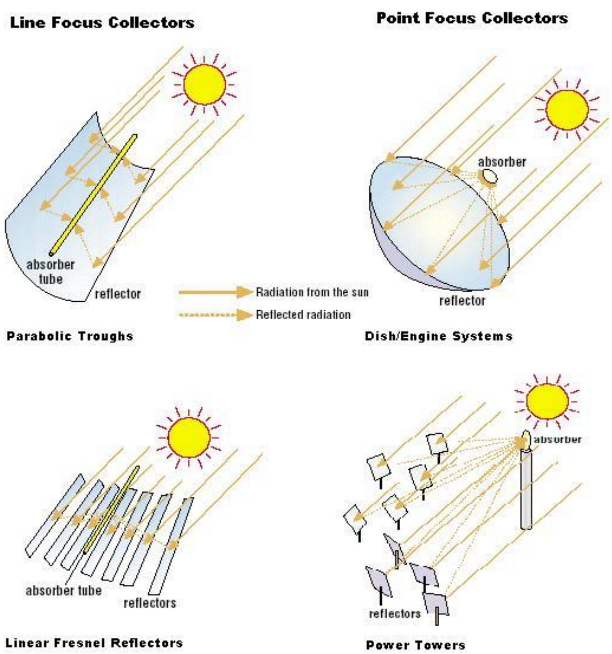

Figure 1 Types of CSP Technologies

NOMENCLATURE

Latin letters

$\overline{n_\lambda}$ = complex index of refraction
n_λ = index of refraction
k_λ = absorptive index
S = path length (m)

Greek letters

$\tau_\lambda(S)$ = optical thickness
β_λ = absorptive coefficient (1/m)
K_λ = absorption coefficient (1/m)
σ_λ = scattering coefficient (1/m)
λ = wavelength (μm)
$\tau_\perp$ = perpendicular component of the transmittance
$\tau_\parallel$ = parallel component of the transmittance
$\rho_\perp$ = perpendicular component of the reflectance
$\rho_\parallel$ = parallel component of the reflectance
$\alpha_\perp$ = perpendicular component of the absorptance
$\alpha_\parallel$ = parallel component of the absorptance
$r_\perp$ = perpendicular component of unpolarized radiation
τ_a = absorption loss
I = local intensity of solar radiation
α = absorptivity
ρ = reflectivity
τ = transmissivity
$\rho_\parallel(\theta_1)$ = parallel component of the reflectivity
$\rho_\perp(\theta_1)$ = perpendicular component of the reflectivity
$\rho_{\lambda,n}(\theta_1)$ = reflectivity for normal incidence

Subscripts

λ = wavelength dependence
⊥ = perpendicular component
∥ = parallel component
a = absorption

SMALL PARTICLE SOLAR RECEIVER

The small particle solar receiver was first introduced by Hunt in the late 1970s [4]. The small particle solar receiver is a large vessel with a window that allows the solar radiation into the receiver. Inside the receiver, a gas-particle suspension flows. This suspension contains air and smoke-like (sum-micron) carbon particles. The solar radiation is absorbed *volumetrically* by the carbon particles. As the carbon particles absorb the solar radiation, the temperature of the particles increases. Therefore, they heat the gas by conduction, which is very effective due to their small size. Eventually, the temperature increase of the suspension causes the carbon particles to oxidize. This process yields a hot, pressurized gas for use in Brayton cycle [4].

The Combustion and Solar Energy Laboratory at San Diego State University is currently working on modeling and designing a 5 MWth small particle solar receiver [5]. The prototype will be built under the SunShot grant awarded by Department of Energy. The small particle solar receiver then will be tested at National Solar Thermal Test Facility (NSTTF).

There have been several numerical simulations of small particle solar receivers. The first study, using a five-flux radiation model, was done by Miller in 1988, who modeled a lower temperature pipe flow system and compared it to lab-scale experiments [6]. In 2010 a detailed radiation study was performed by Steven Ruther, using the Monte Carlo Ray Trace

Copyright © 2013 by ASME

Method and an assumed slug flow fluid dynamics model [7]. The dimensions for the small particle solar receiver in that study were chosen based on an estimate of the heliostat field at the NSTTF. The heliostat field can focus 5 MW solar radiation on a 3 meter diameter circle on the power tower. The window diameter was picked 3 meter based on this fact. A major conclusion of that work was that the receiver was more efficient if the flow was countercurrent to the incoming sunlight.

Later on, this model was improved by Crocker, by adding in a more realistic flow calculation [8]. The geometry of the small particle solar receiver was improved. A schematic of a small particle receiver as modeled by Crocker is shown below in Figure 2 [8]. An outlet tube was added to the receiver with a diameter of 0.6 m. In this research, only counter current flow was studied. The MCRT method was used to solve for the solar radiation and create a source term. A model in FLUENT was built and coupled with MCRT. The source term was generated by the MCRT to the FLUENT model in order to solve energy momentum and mass equations. This process creates a temperature profile which feeds the MCRT. Uniform solar radiation was changed using the Gaussian Flux distribution based on the concentrated solar flux at NSTTF. This provides a more realistic solar energy input. The diameter and the transmissivity of the window were not changed. Other parameters mentioned for Steve's model were not changed and different cases depending on these parameters were studied. The temperature of the working fluid for different cases was varying from 1300K to 1500K [8]. Most recently, the 2-D model of Crocker has been extended to 3-D by del Campo [9]. This will allow coupling of this window and heliostat field model (which are in 3-D) to the receiver model.

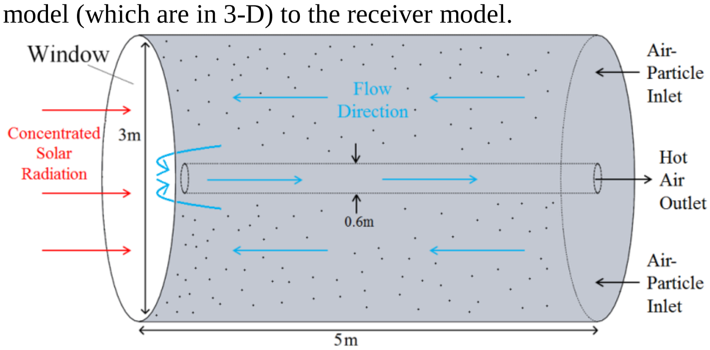

Figure 2 A Schematic of the Improved Small Particle Solar Receiver

There are two main and more realistic window shapes on our focus so that the window will withstand the pressure within the receiver and help minimize the stresses caused by thermal loading as well as the amount of quartz needed.

The first shape is a spherical window with 60 degree cap angle. It is shown that this shape minimizes the amount of the material needed in order to avoid buckling [10]. This shape is easier to manufacture compare to the second shape. The one drawback of this shape is that the tensile stresses near the bottom of the window are not minimized. There are couple of people in CSEL is still working on the seal design for this window shape to handle tensile stresses. In this research, the different cap angles varying from 0 to 90, in other words from flat to hemisphere, for spherical window will be studied.

The second shape is an ellipsoidal shape that Onkar Mande came up with [10]. It has been proven in theory that tensile stresses are eliminated and the entire window is under compression. This shape is harder to manufacture but preferable from a mechanical stand point for quartz. Seal design for this shape is relatively easier. This shape will be compared to the spherical window for their optical performance. The height of the window is the radius of the window times$(\sqrt{2}/2)$.

There are several examples for windowed receivers. One of them is DLR receiver. The receiver is designed for solar-hybrid gas turbine and combined cycle systems and operates at 15 bar. It has a secondary concentrator at the inlet where the solar radiation enters the system right before the quartz window. An absorber is put behind the window. The cold air enters the absorber and gets heated up volumetrically through the absorber then exits the system. The exit temperature of the hot air is between 800 ˚C and 1000 ˚C [11].

Another example is the receiver tested at the Weizmann Institute in Israel (12). The receiver has a quartz flat window and the transmission of the window was measured 87%. Concentrated solar radiation enters the receiver through the window. The radiation is absorbed volumetrically in the receiver by the working fluid that is mixed with carbon particles. Due to thermal stability and high absorption in the entire solar spectrum, carbon particles were chosen to mix with the working fluid. Two working fluids were used: nitrogen and air. The energy flux of the concentrated solar radiation was up to 3 MW/m^2 and the size of carbon particles was around 3 µm in the experiments. The temperature of the working fluid was in between 1343 K and 2118 K depending on the partial pressure ratio of the working fluid, the working fluid type, and the particle loading.

OBJECTIVES OF THIS RESEARCH

One of the purposes of this research is to determine the heating loads that a real window would have and thereby develop a more realistic receiver model. The window, in the models described above, is flat with the transmissivity of 1. As shown by Mande [10], a flat window is not possible in this pressurized situation. Mande discusses concave window shapes that can withstand the pressure by remaining in compression, and these shapes are modeled here optically. Additional modeling of the window as a structural element is currently being reported by Saung [13]. The flat window with a transmissivity of 1 was used in the previous models because those models were developed to study the radiation and fluid dynamics inside the receiver, not the window. In reality, there will be some absorption and reflection at the window surface and this effects what happens inside the receiver. A Fortran code was developed to calculate the optical properties of the window as part of this research. This code accounts for rays

Copyright © 2013 by ASME

reaching the window from arbitrary directions with arbiritary wavelengths.

The other purpose of the research is to have a more realistic solar radiation input. In the models by Crocker and Ruther, the solar input was modeled as either collimated or evenly distributed over a 45 degree cone half angle. In the Ruther model, there was no spatial variation across the aperture plane, while in the Crocker model a Gaussian distribution was considered. In reality, however, the direction of the radiation will be different depending on the day of the year, time, location of the receiver, and the heliostat field, etc. MIRVAL is modified and used to consider all these affects in order to get a realistic solar radiation input.

MONTE CARLO RAY TRACE METHOD

The Monte Carlo method is a statistical approach to investigate problems by creating applicable random numbers and considering probability distributions. The Monte Carlo method was first used in radiation heat transfer (the Monte Carlo Ray Trace) in 1964 by Howell and Perlmutter [14]. One-dimensional gray participating media between infinite parallel plates was considered in the paper. The method was applied to this case and the results were validated against the conventional approach. It was mentioned in the paper that the MCRT method can be used easily in more complex cases which can be difficult to solve by standard analytical techniques [14]. Later on, complex cases were investigated by Howell [15]. The results have shown that the MCRT method is flexible enough to be applied to the complex case but the computation time gets longer as the case gets more complex. MCRT method has also been proven that it can be adapted to parallel computation which will reduce the computation time. Also, computing time is becoming a less of an issue as the computer technology is developing [15].

Several computer codes have been built to calculate the solar flux concentration in concentrated solar power systems, and two of these use the MCRT method [16]. One of them is called MIRVAL. MIRVAL was developed for optical performance analysis for Solar One project by Sandia National Laboratories [16]. The flux calculation from heliostat filed to the power tower is essentially a radiation exchange from surface to surface. A same method is used to calculate the radiation that is transmitted by the window to the receiver.

MIRVAL

As it was mentioned earlier, MIRVAL is a computer code developed by Sandia National Laboratories in 1979. MIRVAL is obtained by personal communication from Cliff Ho [17]. MIRVAL is capable of computing the solar thermal input to a solar receiver from heliostats as well as simulating and evaluating the performance of different heliostats by using the MCRT method. It was first used in order to evaluate competing designs for Solar One project. Under the Solar One project, a 10 MW pilot plant was built near Barstow, California [18].

MIRVAL offers many subroutines that are already built in, for different types of heliostats and power towers. Since MIRVAL is handling the calculations for heliostats and power towers in the subroutines, it is easy to modify the necessary subroutine in order to apply MIRVAL for different designs that need to be investigated.

Appropriate subroutines were picked and modified in order to simulate NSTTF. The map of heliostat field is shown below in Figure 3. The map was provided by Cliff Ho from Sandia National Laboratory via personal communication. This field was mapped in MIRVAL as well as defining the size and the material properties of the mirrors.

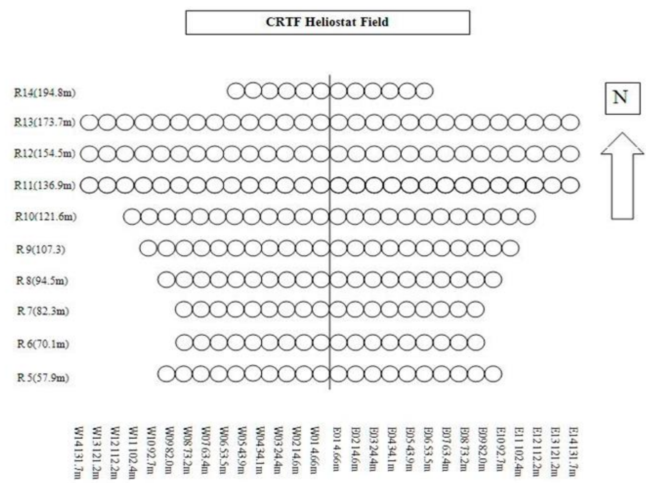

Figure 3 Map of Heliostat Field at NSTTF

There are several input variables which represent the location of the aperture [18]. These variables were chosen according to the NSTTF sizes. The height of the aperture plane is 60 m and has a tilt angle of 23.8˚ from the vertical. This angle was chosen to aim the aperture to the middle of heliostat field.

There are several reasons why the flux map at the aperture plane is needed. One of the reasons is to have a better understanding of how well the concentrated flux is focused. Another reason is to figure out the location of the highest concentration and how it changes throughout the day. Last but not the least, the value of the highest flux can be determined. The rays are then traced beyond the aperture plane until they meet the window which is behind the aperture plane unless the window is flat.

The following three figures are the flux maps for different times on March 21st. March 21st is the first equinox day of the year. The purpose is to get a better concentration at the origin of the aperture plane. The radius for the aperture plane (not the window) was picked to be 1.5 m for illustrative purposes. There are rays that falls out of this range. They were not considered because the number of these rays is negligible.

Copyright © 2013 by ASME

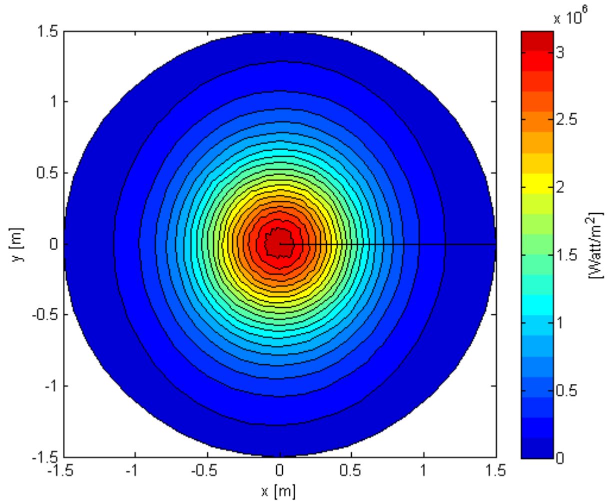

Figure 4 Flux Map at 12 pm on 3/21 with 23.8˚ Tilt Angle

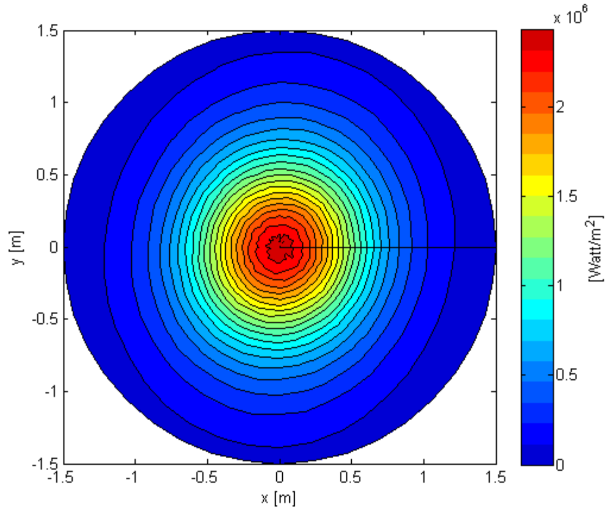

Figure 5 Flux Map at 2 pm on 3/21 with 23.8˚ Tilt Angle

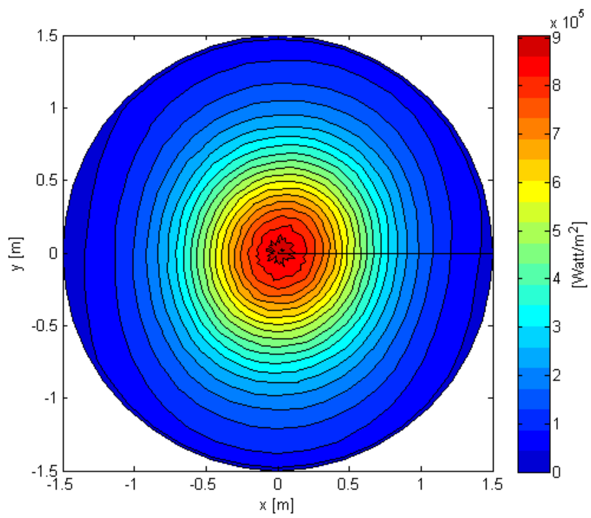

Figure 6 Flux Map at 4 pm on 3/21 with 23.8˚ Tilt Angle

Among the studied times, the highest heat flux is reached at 12 pm and the value of it is 3.2 MW/m^2. The lowest heat flux is reached at 4 pm and the value of it is 0.9 MW/m^2. The change in time does not have a significant effect on the location of the highest heat flux concentration but the change in power is drastic. Therefore, this change should be investigated more carefully.

Figure 7 has been created to show how much power is captured on the aperture plane with respect to the radius. Three different times were studied. It can be easily seen among the chosen times the power is higher at 12 pm and lower at 4 pm. The bigger radius at the aperture plane will have a bigger surface area and that will allow more light capture, although it will also increase the receiver losses.

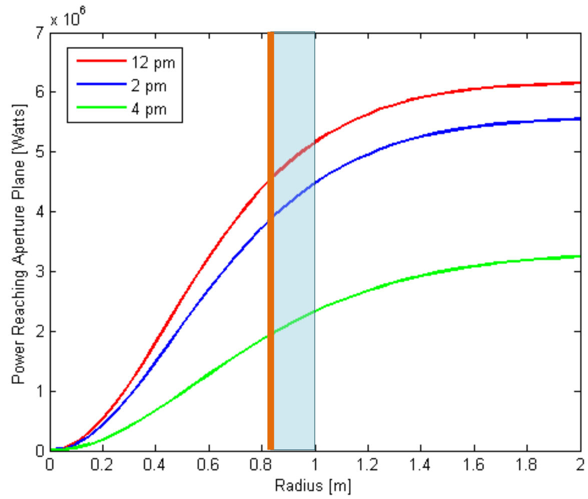

Figure 7 The Power Reaching the Aperture Plane vs. Radius

The window for the solar receiver will be located where the aperture plane is in order to let the solar radiation inside the solar receiver. It is obvious, only by looking at Figure 7, that if the radius of the window is bigger than more radiation will enter the receiver. More radiation means more energy captured inside the receiver. The bigger radius will create some issues. One of the issues is that there will be radiation coming from inside of the receiver and leaving the receiver from the window, representing radiation losses. Without a detailed receiver model coupled to the window model, it is not possible to determine the optimal window diameter, though clearly the advantages of a larger window begin to decrease at about 1 m. This is something under current research by our group. The other issue is high cost of quartz, and of fabricating large quartz windows, currently being studied by Saung [13]. All of these factors should be studied very carefully in order to find the optimum radius for the window. Here we consider the solar flux on the window, but not the window cost or the losses from the inside the receiver. For our base case, the radius for the window will be picked as 0.85 m (orange line in Figure 7). The radius (at the aperture plane) is picked according to the power that will be let into the receiver from the heliostat field, 5 MWatt. We, the Combustion and Solar Energy Laboratory at San Diego

Copyright © 2013 by ASME

State University, are interested in window radius up to 1 m (blue rectangular in Figure 7)

OPTICAL PROPERTIES OF THE WINDOW

The heliostat field reflects the sun light to its focal point where the window of the small particle solar receiver is located. There are several processes that will occur at the window after the sun light hits the window. The light can be reflected from the first interface of the window and can hit the window again or leave the system. The light can also get through the first interface and be absorbed by the window, or it might reach the second interface of the window. After reaching the second interface two different possibilities might occur. One is the light might get transmitted through the window and enters inside the solar receiver. Second is the light might be reflected back. The reflected light might be absorbed by the window or might reach the first interface. Later it might get transmitted and leave the system or might be reflected back to the window and the same incidents might occur. Figure 8 shows all the possible incidents that might occur at the window.

The absorptivity, the reflectivity, and the transmissivity of the window are needed in order to determine the fate of the light at the window.

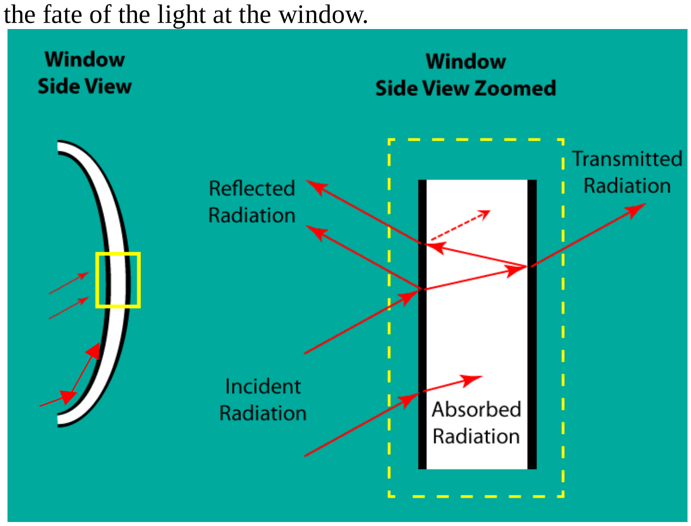

Figure 8 The possible interactions of radiation with the window.

These optical properties are a function of the wavelength and direction of the incoming radiation, and the index of refraction and the absorptive index of the material, in this case quartz.

Much research has shown that quartz is a selective material which has a high transmissivity in the solar spectrum. Selective material means that the material behaves differently depending on the wavelength of the incident radiation. Incoming radiation from the heliostat field will be in the solar spectrum. Therefore, high transmissivity in the solar spectrum is needed in order to let as much as radiation inside the receiver. This is the reason why quartz was chosen for the material of the window. The solar spectrum range is in between 0.2 um to 2.5 um.

THE INDEX OF REFRACTION AND THE ABSORPTIVE INDEX

Fused quartz is an imperfect dielectric material. A perfect dielectric material does not absorb incident radiation. Fused quartz glass, like all real materials, does absorb some incident radiation due to OH^- and metallic impurities. The amount it absorbs depends strongly on the wavelength and also on the thickness of the glass. In such a material, the incident radiation (electromagnetic waves) is attenuated as it passes through the medium. Attenuation in the medium is expressed by replacing the index of refraction of the medium with a complex index of refraction $\bar{n}$. The imaginary part k_λ is called the absorptive index and n_λ is called the index of refraction [19].

$$\overline{n_\lambda} = n_\lambda - ik_\lambda \tag{1}$$

The index of refraction and the absorptive index are needed to determine the optical properties such as the absorptivity, the reflectivity, and the transmissivity. The index of refraction is the ratio of the speed of light in the vacuum and in the medium. The absorptive index is a measurement of how radiation gets absorbed in the medium. They are both function of the wavelength of the radiation and the temperature of the material. The data for these two properties are an excerpt from Dr. Laurent Pilon's research [20]. In the paper, it is shown that most of the experiments are done at room temperature. The effect of the temperature on these properties is not as significant as wavelength.

Much research has been done on the index of refraction and the absorptive index [20]. The data has been reviewed within a wavelength range of 0.1 um to 50 um. Most of the values of the absorptive index and the index of refraction in a particular wavelength match in different researches or they are close enough. But in some of the research papers the data are not in agreement. The outliers are taken off and the data that are in somewhat agreement are used to obtain a smooth data set which is necessary to get accurate polynomial fit equations as well as the wavelength range. At last, Figure 9 is reached. The effects of the wavelength differ greatly with regard to the index of refraction and the absorptive index as it is seen in the graphs. It is important to find the appropriate wavelength range. Considering these two facts, the polynomial fit equations are found. These polynomial fit equations are used to find the absorptive index and the index of refraction depending on the wavelength in the following calculations.

Copyright © 2013 by ASME

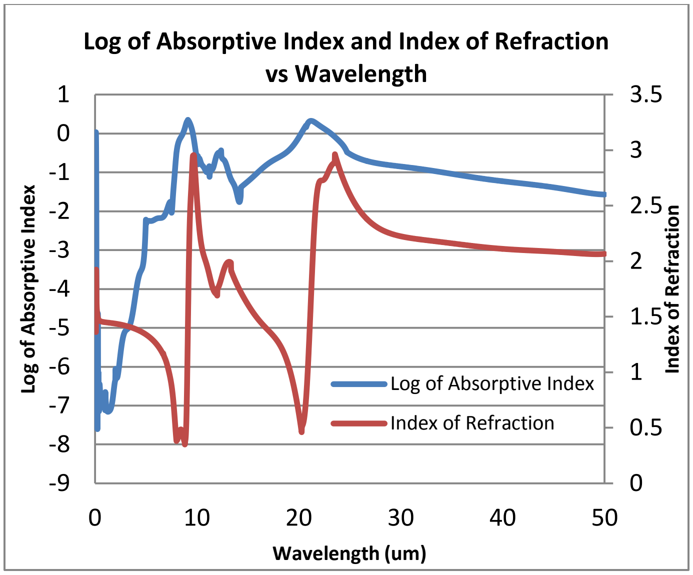

Figure 9 Log of Absorptive Index and Index of Refraction by Using Data from Dr Pilon's Research

THE OPTICAL THICKNESS

The optical thickness is a dimensionless quantity, denoted as $\tau_\lambda(S)$. It is also called opacity along the path length S. The attenuation on the radiation at a given wavelength is simply indicated by the optical thickness. If the optical thickness is much bigger than 1, the medium is called optically thick which means that the radiation does not go through the medium instead it is absorbed by the medium. If the optical thickness is much smaller than 1, the medium is called optically thin which means that the radiation goes through the medium. As the optical thickness gets bigger, the medium will become opaque and in contrast to this, the medium will become less participating as the optical thickness gets smaller and eventually the medium will become perfectly transparent [19].

$$\tau_\lambda = \int_0^S \beta_\lambda(S^*)dS^* \tag{2}$$

Glass is a medium with uniform properties, therefore Equation 2 becomes

$$\tau_\lambda(S) = \beta_\lambda S \tag{3}$$

$$\beta_\lambda = K_\lambda + \sigma_\lambda \tag{4}$$

In Equations 2 and 3, S is the path length that the radiation travels on and β_λ is absorptive coefficient which represents the attenuation on the radiation that is traveling in the medium. The attenuation can be caused by absorption or scattering. In Equation 1.4, K_λ is the absorption coefficient and σ_λ is the scattering coefficient. Since the glass does not scatter the radiation (assuming bubbles and other inclusions are negligible), Equation 3 becomes

$$\tau_\lambda(S) = K_\lambda S \tag{5}$$

K_λ, the absorption coefficient, is a function of the wavelength and the absorptive index [19]. It varies drastically with the wavelength. It also varies with the temperature and the pressure, though not as strongly. The data for k_λ for a given wavelength is taken from the polynomial fit equations that are created from the data collected from Dr. Laurent Pilon's research as was mentioned earlier.

$$K_\lambda = \frac{4\pi k_\lambda}{\lambda} \tag{6}$$

THE ABSORPTIVITY, THE REFLECTIVITY, AND THE TRANSMISSIVITY

Depending on the value of the optical thickness, two sets of formulas were used to determine the absorptivity, the reflectivity and the transmissivity. One is called low opacity method and the other is high opacity method.

Low Opacity Method:

Low opacity method is used when the absorptive coefficient is very small. When the absorptive coefficient is very small the optical thickness will be small too. In this case, low opacity, the effect of absorptive index can be negligible from the complex index of refraction. Therefore Equation 1 becomes

$$\overline{n_\lambda} = n_\lambda \tag{7}$$

Snell's law, which describes the relationship in between the angle of incident radiation and the angle of refraction, is given by Equation 8 [19]. Subscripts 1 and 2 represent different media. 1 is air and 2 is the glass in our case. The index of refraction is 1 and the absorptive index is approximately 0 for the incident radiation in the air.

$$\frac{\sin\theta_2}{\sin\theta_1} = \frac{\overline{n_1}}{\overline{n_2}} = \frac{n_1 - ik_1}{n_2 - ik_2} \tag{8}$$

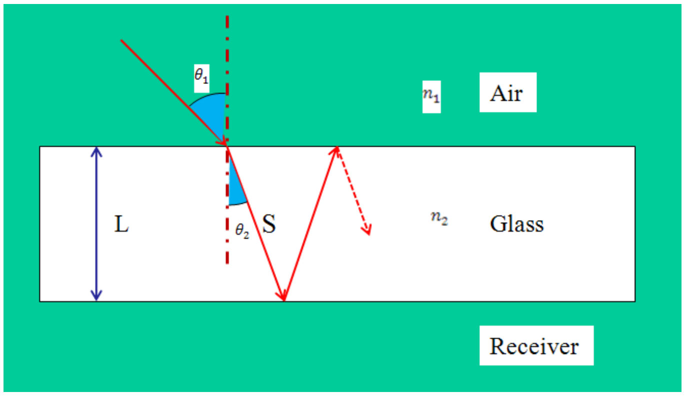

Figure 10 Angles of Incoming Radiation and Refraction

Copyright © 2013 by ASME

θ_1 is the angle of incoming radiation and θ_2 is the angle of refraction, shown in Figure 10.

The perpendicular component of the transmittance, the reflectance, and the absorptance of a single sheet of glass, which is one of the faces of the window in this case, can be obtained either by the net radiation method or by ray tracing methods. The perpendicular component of the transmittance ($\tau_\perp$), the reflectance ($\rho_\perp$), and the absorptance ($\alpha_\perp$) of a single glass sheet are shown in Equation 9 to 11. $r_\perp$ represents the perpendicular component of unpolarized radiation, derived by Fresnel. Similar results are found for the parallel component of polarization [14]. τ_a is described in Equation 13. Here, parallel and perpendicular components represent the direction of the electric fields of the rays.

$$\tau_\perp = \frac{\tau_a(1-r_\perp)^2}{1-(r_\perp\tau_a)} = \tau_a\frac{1-r_\perp}{1+r_\perp}\left[\frac{1-r_\perp{}^2}{1-(r_\perp\tau_a)^2}\right] \tag{9}$$

$$\rho_\perp = r_\perp(1+\tau_a\tau_\perp) \tag{10}$$

$$\alpha_\perp = (1-\tau_a)\left(\frac{1-r_\perp}{1-r_\perp\tau_a}\right) \tag{11}$$

Bouguer's law describes the absorption of incoming radiation in a partially transparent medium such as glass. It is assumed that the absorbed radiation and the local intensity in the medium are proportional to each other. It is given in Equation 12.

$$dI = -IK_\lambda\, dx \tag{12}$$

K_λ is the absorptive coefficient. x is the path length that radiation travelled in the medium. Integrating Equation 12 in the medium along the path length of S lead us to

$$\tau_a = \frac{I_{transmitted}}{I_{incident}} = exp(-K_\lambda S) \tag{13}$$

$$S = \frac{L}{\cos\theta_2} \tag{14}$$

Where τ_a is absorption loss and K_λ is absorptive coefficient as it was mentioned before. L is the thickness of the glass. θ_2 is the refraction angle [21]. The path length S is different for each ray depending on the incident angle, indices of refraction of the two media, and the thickness of the glass. Absorption loss will increase as S increases. S is also shown earlier in Figure 10.

Finally the transmissivity, absorptivity and reflectivity for the low opacity case are found by averaging the parallel and the perpendicular components of polarization. They are given in Equation 15 to 18. Since these optical properties are the percentages, they should add up to one [21].

$$\tau = \frac{\tau_\perp + \tau_\parallel}{2} \tag{15}$$

$$\rho = \frac{\rho_\perp + \rho_\parallel}{2} \tag{16}$$

$$\alpha = \frac{\alpha_\perp + \alpha_\parallel}{2} \tag{17}$$

$$\alpha + \rho + \tau = 1 \tag{18}$$

High Opacity Method:

In the case of high opacity, which means the optical thickness is much bigger than 1, the absorptive index is high enough that it cannot be negligible in developing the interface reflectivities. The formulas that are given before in order to calculate the optical properties of the glass have the dependency of the refraction angle. Therefore they cannot be used. However, the glass can be treated as an opaque absorbing medium. The reason is that in this case, there will be no transmission since the medium is optically thick. The radiation can be either reflected or absorbed. The parallel and perpendicular components of the reflectivity are given in Equation 19 and 20 for an absorbing medium that is exposed to the radiation coming from air [19].

$$\rho_\parallel(\theta_1) = \frac{(n_2\gamma - \alpha/\cos\theta_1)^2 + (n_2^2+k^2)\alpha - n_2^2\gamma^2}{(n_2\gamma + \alpha/\cos\theta_1)^2 + (n_2^2+k^2)\alpha - n_2^2\gamma^2} \tag{19}$$

$$\rho_\perp(\theta_1) = \frac{(n_2\beta - \cos\theta_1)^2 + (n^2+k^2)\alpha - n^2\beta^2}{(n_2\beta + \cos\theta_1)^2 + (n^2+k^2)\alpha - n^2\beta^2} \tag{20}$$

Where

$$\alpha^2 = \left(1 + \frac{\sin^2\theta_1}{n_2^2+k^2}\right)^2 - \frac{4n^2}{n_2^2+k^2}\left(\frac{\sin^2\theta_1}{n_2^2+k^2}\right) \tag{21}$$

$$\beta^2 = \frac{n_2^2+k^2}{2n_2^2}\left(\frac{n_2^2-k^2}{n_2^2+k^2} - \frac{\sin^2\theta_1}{n_2^2+k^2} + \alpha\right) \tag{22}$$

$$\gamma = \frac{n_2^2-k^2}{n_2^2+k^2}\beta + \frac{2n_2k}{n_2^2+k^2}\left(\frac{n_2^2+k^2}{n_2^2}\alpha - \beta^2\right)^{1/2} \tag{23}$$

As it is seen in the equations, there is no refraction angle dependency. The reflectivity is a function of the index of refraction, the absorptive index and the incident angle.

The reflectivity for the high opacity case is found by averaging the parallel and the perpendicular components. The absorptivity will be 1 minus the reflectivity since the transmissivity is 0 in this case.

$$\rho = \frac{\rho_\perp + \rho_\parallel}{2} \tag{24}$$

$$\alpha = 1 - \rho \tag{25}$$

$$\tau = 0 \tag{26}$$

For the radiation that hits the interface at normal incidence, the reflectivity is given in Equation 27 (19).

$$\rho_{\lambda,n}(\theta_1) = \frac{(n_2-n_1)^2 + (k_2-0)^2}{(n_2+n_1)^2 + (k_2+0)^2} \tag{27}$$

Copyright © 2013 by ASME

RESULTS FOR OPTICAL PROPERTIES

The program called optical_properties_TD has been written by using Fortran in order to calculate the optical properties of the glass window, which are the transmissivity, absorbtivity and reflectivity. The wavelength range that is used for the calculation purposes is in between 0.1 um to 50 um. This wavelength range is chosen in order to match the developed code to the previous code that was created by Steven Ruther for the receiver. In his work, it was explained that the upper wavelength cutoff can be chosen so that the excluded black body fraction is negligible. The approximate wall temperature of the small particle solar receiver is 1000 K. The chosen upper wavelength cutoff is 50 μm. The reason to choose this number is that only 0.11 % of the black body fraction is excluded. This is a very small portion and is negligible [7].

It was mentioned earlier that the optical thickness is a dimensionless number that defines the opacity of the material. If the optical thickness is much bigger than 1 then the medium is optically thick. This cutoff number, optical thickness also called critical opacity, is very important to find since there are two different approaches to find the transmissivity, absorptivity, and reflectivity depending on this number as explained in the section called the absorptivity, the reflectivity, and the transmissivity, . The effect of the critical opacity on the optical properties was studied to pick the right number. The critical opacity was varied from 1 to 15. The wavelength and the incident angle of the incoming radiation and the thickness of the glass are the three important variables that have a tremendous effect on the optical properties such as the absorptivity, the reflectivity, and the transmissivity. The incident angle was varied from 0 degree to 75 degree on a 2.5 cm thick window while the wavelength was varied from 0.1 μm to 50 μm.

The results of the studies showed that the effect of the critical opacity for the optical thickness is significant in the wavelength interval of approximately 3 μm to 4.6 μm, depending on the other parameters mentioned earlier. In this wavelength interval, the transition of the glass from being transparent to being opaque can be seen. Only one figure is displayed to show the effect of the critical opacity on the absorptivity. Similar results are observed for the transmissivity and the reflectivity. The displayed figure is only for one specific incident angle because a change in incident angle will of course change the values of optical properties, but the effect of the critical opacity is same for different incident angles. Therefore, similar results are also observed with various angles for the transmissivity and the reflectivity.

The significant effect of the critical opacity on the optical properties can be easily seen on Figure 11. The figure is for a 2.5 cm thick window with 0 degree incident angle. There is a very unrealistic jump from absorptivity of approximately 0.6 to 0.98 in both figures. The area between the red line and the blue line in each figure is the extra absorption that is considered when the critical opacity is chosen 1. Extra absorption will show a temperature increase in window temperature when that is eventually calculated. The yellow line in the figures cannot even be seen because 10 and 15 leads the same results. The lines are very smooth and realistic. Therefore, either 10 or 15 can be chosen for the critical opacity. 10 will be used for the calculations.

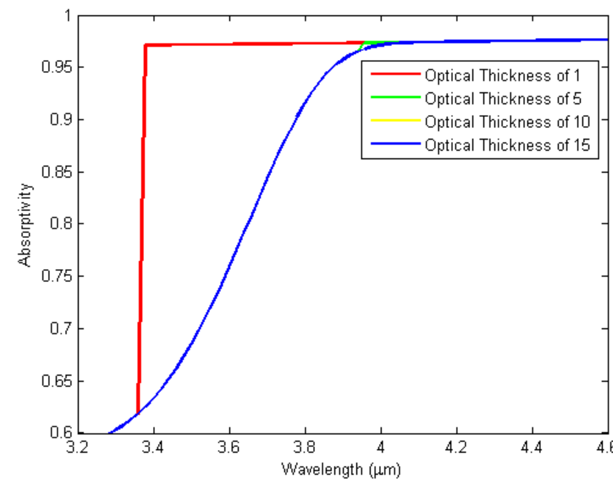

Figure 11 The Effect of the Critical Opacity Number on Absorptivity for 2.5 cm Thick Window with 0 Degree Incident Angle

Now that the critical opacity is chosen, further calculations can be performed to find the solutions for optical properties. The results for the optical properties will also be displayed for 2.5 cm thick window. The incident angle of the incoming ray has a significant effect on the results, therefore, will be defined for each figure. The full wavelength range for this research (0.1 μm to 50 μm) will be studied as well as solar spectrum.

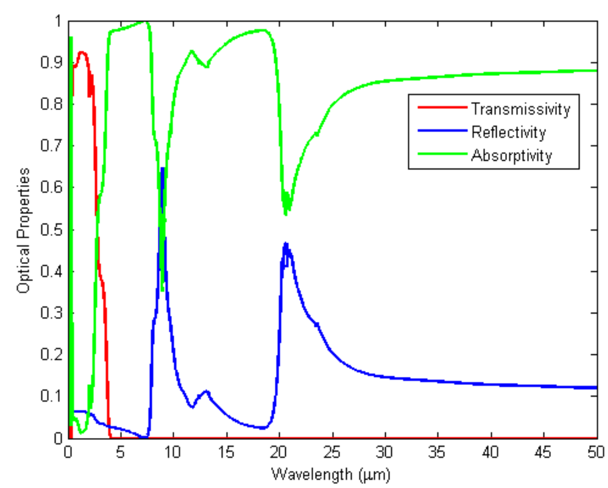

Figure 12 Optical Properties of the Window (2.5 cm thick, 0 degree incident angle)

It was mentioned before that quartz is a selective material which has a high transmissivity in the solar spectrum. Figure 12 supports this statement. The transmissivity of the quartz window is over 90% in the solar spectrum.

 Copyright © 2013 by ASME

Approximately 3% of absorption and 6% of reflection is also observed in the solar spectrum. The transmissivity drops to 0 percent around 4 μm. In the longer wavelengths, high absorptivity, lower reflectivity, and no transmissivity are encountered.

The effect of incident angle on the optical properties cannot be easily seen in Figure 13 despite the change in incident angle. The change in the optical properties is more obvious as the incident angle increases. This change can be seen in Figure 14 when the incident angle is 60 degree. It was observed that the transmissivity of the window decreases while the reflectivity increases. The absorptivity behaves differently depending on the wavelength of the incoming ray because the change in the absorptive coefficient is very rapid depending on the wavelength.

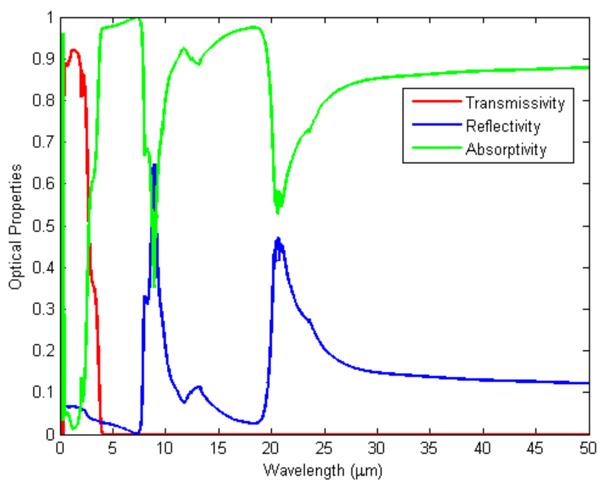

Figure 13 Optical Properties of the Window (2.5 cm thick, 30 degree incident angle)

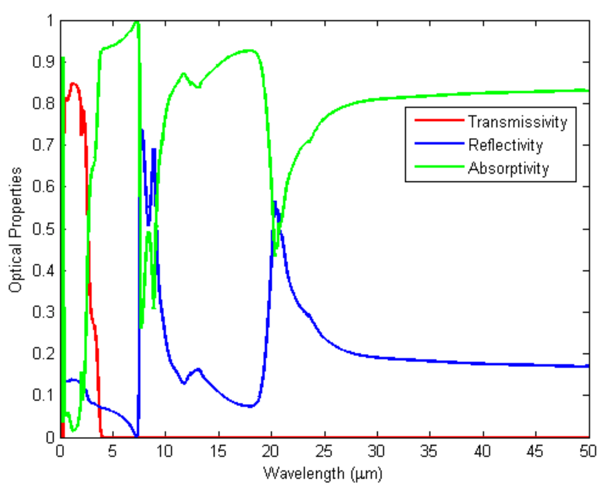

Figure 14 Optical Properties of the Window (2.5 cm thick, 60 degree incident angle)

Optical properties were plotted with respect to the incident angle for a chosen wavelength in order to have a better understanding of the effect of the incident angle on the optical properties. The thickness of the window was kept the same as 2.5 cm while two different wavelengths were studied. The peak of solar spectrum is 0.5 μm and the maximum spectral blackbody emissive power from the receiver is reached at approximately 3 μm. Therefore, these two wavelengths were chosen for the study.

The results show that the effect of the incident angle on the optical properties is more obvious after 40 degree incident angle. The transmissivity decreases, the reflecticity increases, and the absortivity first increases then decreases, shown in Figure 15 and Figure 16. These incidents always occur despite the wavelength of the incoming radiation, although the magnitude can vary.

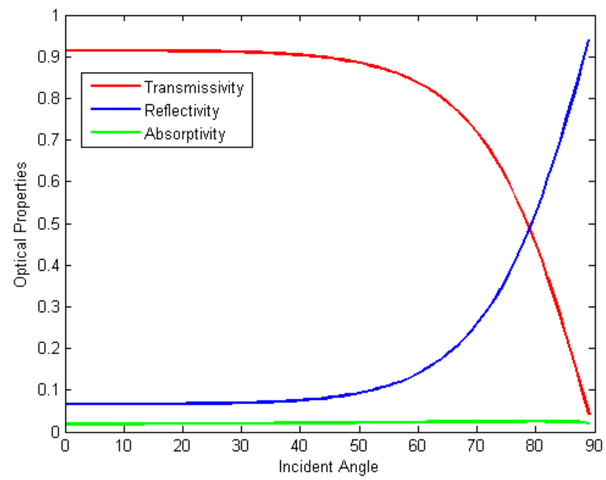

Figure 15 Optical Properties of the Window (2.5 cm thick, 0.5 μm)

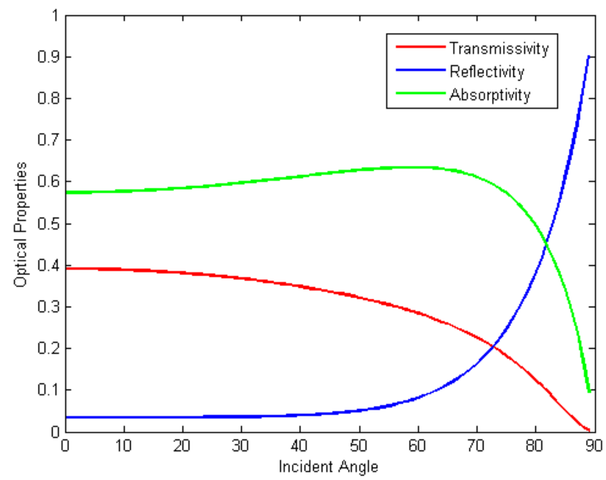

Figure 16 Optical Properties of the Window (2.5 cm thick, 3 μm)

The calculations, by using the data we have, led us to results that showed higher absorptivity and somewhat lower transmissivity in the solar spectrum. The lower the absorptivity and the higher the transmissivity is, the better for a solar receiver. The main purpose is to get as much as radiation into

Copyright © 2013 by ASME

the receiver with absorbing the least amount of radiation by the window since absorbed radiation will heat the window up over the operating temperature. Therefore, the optical properties should be investigated closely.

Looking deep into the Dr. Pilon's paper and looking at his references, it is concluded that the papers do not show enough information about the quartz material such as metal impurity, OH- content etc. Therefore, the quality of the quartz studied in the paper is unknown. More data are needed to compare the results in order to choose the right material. Since the window will actually be built soon, we contacted our vendor Heraeus to obtain more realistic data. Some data for the optical properties in different wavelength were provided for comparision, also can be found in reference [22]. Figure 17 show the comparison of absortive indices for different types of materials. The lower absorptive index will lead to lower absorption, therefore, higher transmission. By looking at Figure 17, Surprasil 3001 looks like a great choice for the material without considering the cost of the window.

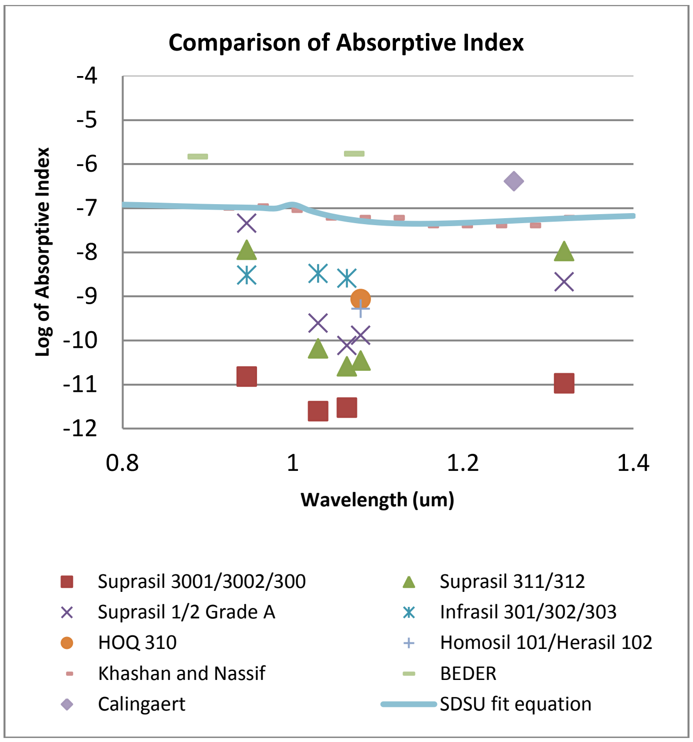

Figure 17 Comparison of Absorptive Indices

RAY TRACE AT THE WINDOW

Accurate modeling for radiation heat transfer in between surfaces with a nonparticipating medium can be done regarding the type of the surfaces by using diffuse transfer analysis or exchange of thermal radiation among nondiffuse nongray surface method [19, 23]. Geometric view factors for each method are needed as input parameters. These view factors can be very difficult to define when complex geometries are involved. The term nondiffuse means the directional emissivity and the directional absorptivity depend on direction. Nongray means the spectral emissivity and the absorptivity depend on wavelength [19]. The quartz window is a specular, nongray surface.

The Monte Carlo method is another approach for solving radiation heat transfer in between surfaces. It is a statistical approach that uses probability concepts to create models for physical events. The Monte Carlo Ray Trace (MCRT) method includes physical events such as photon emission, reflection, absorption, and transmission. It involves tracing rays of photon bundles from the source of emission or reflection through a nonparticipating media until they are absorbed by a surface or they leave the problem domain. The direction of the rays and the physical events when a ray encounters a surface is determined by generated random numbers compared with appropriate probability functions. To sum up, there are two main steps to this method. First step is to create appropriate rays each assigned with a power, and a direction. The second step is to track these rays and keep a tally of the rays that are leaving the problem domain or absorbed.

These steps are done in MIRVAL for the heliostat field. MIRVAL creates imaginary rays leaving the sun assigned with power. These rays travel through air which is a nonparticipating medium (for the analysis run here) and reach the heliostat field. Then, some reflected rays from the heliostat field reach the power tower as shown in the earlier figures. These two steps constitute the first step of MCRT on the window. The direction, the location at the power tower, and the power of each ray that reached the power tower is recorded. Therefore, these data are the first step of MCRT on the window.

There is one addition to these steps in case of a nongray surface (window). Spectral analysis need to be done for nongray surfaces which means the wavelength of the rays need to be known. MIRVAL does not include the spectral analysis since the heliostats are treated as a gray surface. Therefore, we modified the program to account for wavelength.

A computer code called window_TD was developed, by using the MCRT method, to trace the rays that are incident on the window as they get absorbed reflected or transmitted by the window. Reflected rays were traced until they leave the problem domain or absorption or transmission occurs.

There are two main window shapes being considered so that the window will withstand the pressure within the receiver and help minimize the stresses caused by thermal loading as well as the amount of quartz needed. The first shape is a spherical window and the second shape is an ellipsoidal window.

Some results were obtained by running window_TD using 100 million rays. Figure 18 and Figure 19 show the absorption on the window from only the solar radiation coming from the heliostat field. The window is a 60 degree hemispherical cap and the radius of the curvature is 0.98 meters which corresponds to 0.85 m radius at the aperture plane. The highest heat flux is near the center of the window with an approximate value of 0.44 MW/m^2.

Copyright © 2013 by ASME

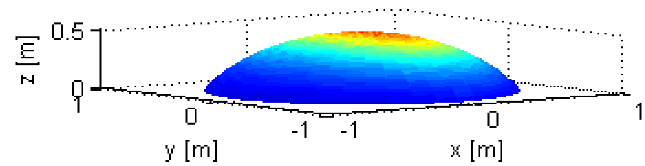

Figure 18 Flux Map of Absorbed Radiation at the Window on March 21st at 12 pm for 2.5 cm thick window

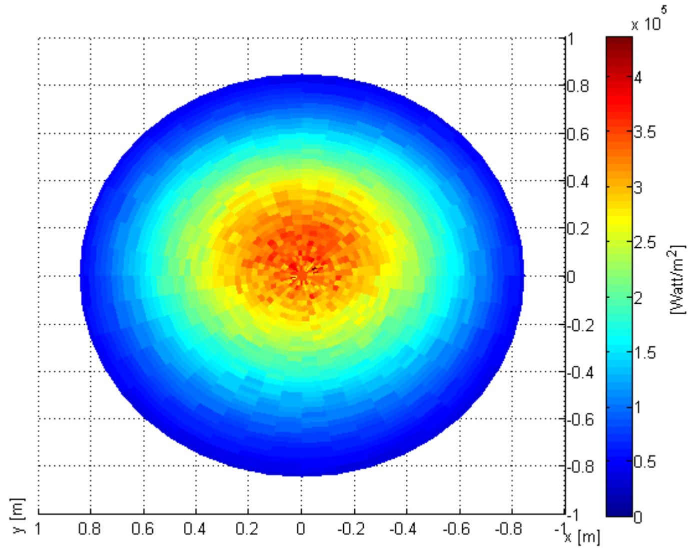

Figure 19 Top View for the Flux Map of Absorbed Radiation at the Window on March 21st at 12 pm for 2.5 cm thick window

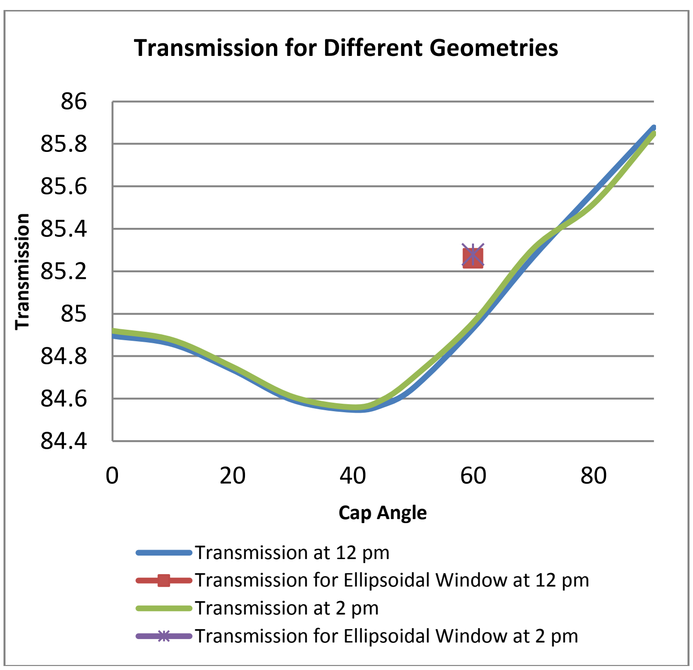

Figure 20 Transmission for Different Geometries at 12 pm and 2 pm

Figure 20 shows the transmission for both a spherical cap and an ellipsoidal window. The radius for both windows is 0.85 m. The thickness is 2.5 cm and the number of rays used is 16 million. Results show that the effect of cap angle is important and affects the transmissivity. As the cap angle increases, the transmission starts to decrease up to approximately a 45 degree angle then it starts to increase. The hemispherical window, 90 degree cap angle, shows the highest transmission. The ellipsoidal window and the 70 degree spherical window have approximately the same transmission. The change in time of day doesn't have a significant effect on the transmission.

The reason why there is a decrease in transmission for lower cap angles is that the incident angle of the rays that are hitting the window will be different for different cap angle windows. Therefore, the value of reflectivity will be different. Last but not the least, the rays that are reflecting from the window will have higher chances to hit the window again when the cap angle is higher. This explains the increase in transmission for higher cap angles.

CONCLUSION

Several computer programs have been developed and modified to do optical analysis on the window for small particle solar receiver. Although applied here to a particle receiver, any windowed receiver can be modeled in this way. MIRVAL was modified to calculate the solar radiation coming from the heliostat field to the aperture plane on the power tower. Window_TD was developed to track the rays after the aperture plane until they get absorbed or transmitted or reflected (until the ray leaves the problem domain). Window_TD is coupled with optical_properties_TD .optical_properties_TD calculates the optical properties of the window such as the tranmissivity, the absorptivity, and the reflecticity. Window_TD uses these properties to find the fate of the ray. Many data that are needed have been stored for the optical analysis.

The results showed a lower transmissivity and a higher absorptivity than expected. High absorptivity will lead to an increase in window temperature while operating. That might cause the window to crack due to differential thermal expansion. The high absorptivity found here is directly related to the absorptive index found for the quartz. The values of absorptive index we currently have from the literature are very high. Better values for a better kind of quartz are needed for the wavelength range of 0.3 μm to 15 μm in order to get more realistic results for the window absorption. Right now, we are trying to get more data for additional types of quartz to complete our optical analysis.

ACKNOWLEDGMENTS

The authors acknowledge the support by the Department of Energy with its SunShot program under the Award # DE-EE0005800. We also thank Andrew Clarkson from L-3 Brashear, and Dr. Arlon Hunt for their helpful discussions and commentary on this research, and Cliff Ho of Sandia National Laboratory for providing MIRVAL. The authors also would like to thank their colleagues in C&SEL.

Copyright © 2013 by ASME

REFERENCES

[1] http://www.volker-quaschning.de/articles/fundamentals2/index.php. *Technology Fundamentals: Solar Thermal Power Plants.* [Online]
[2] Robinson, Jess and Romero, Yuber. *Concentrating Solar Power Clean Energy for the Electric Grid.* Boston : Mcgraw-Hill/Irwin, 2008.
[3] International Renewable Energy Agency. Renewable Energy Technologies: Cos Analysis Series. June 2012, Vol. 1, Power Sector 2/5.
[4] *A New Solar Thermal Receiver Utilizing Small Particles.* Arlon, J Hunt. Atlanta, GA : Proc. Int. Solar Energy Society Conf., 1979. pp. 1362-1366.
[5] *Developing the Small Particle Heat Exchange Receiver for a Prototype test.* Miller, Fletcher J. and Hunt, Arlon J. San Diego, CA : ASME 2012 6th International Conference on Energy Sustainability, 2012.
[6] *An Experimental and Theoretical Study of Heat Transfer in a Gas-Particle Flow Under Direct Radiant Heating.* Miller, Fletcher. Berkeley, CA : Department of Mechanical Engineering, University of Berkeley, 1988.
[7] Ruther, Steven James. *Radiation Heat Transfer Simulation of a Small Particle Solar Receiver Using the Monte Carlo Method.* San Diego, CA : San Diego State University, 2010.
[8] Crocker, Adam Winfield. *Coupled Fluid Flow and Radiation Modeling of a Small Particle Solar Receiver.* San Diego, CA : San Diego State University, 2012.
[9] *Three-Dimensional Fluid Dynamics and Radiative Heat Transfer Modeling of a Small Particle Solar Receiver.* Croker, Adam, Miller, Fletcher and Fernandez del Campo, Pablo. Minneapolis, MN : ASME, 2013. 18149.
[10] Mande, Onkar Kiran. *Window Seal Design for a Small Particle Solar Receiver.* San Diego, CA : San Diego State University, 2011.
[11] *Test and Evaluation of a Solar Powered Gas Turbine System.* Heller, P., et al., et al. s.l. : Solar Energy, 2006, Vol. 80. pp. 1225-1230.
[12] *Experimental Evaluation of Particle Consumption in a Particle Seeded Solar Receiver.* Helena, K. H., Rubin, R. and Karni, J. Seviller, Spain : Solar PACES International Symposium, June 2006.
[13] *Dome Window and Mount Design for a Large Scale Solar Receiver.* Saung, E-fann and Miller, Fletcher. Minneapolis, MN : ASME, 2013. 18217.
[14] *Monte Carlo Solution of Thermal Transfer Through Radiant Media Between Gray Walls.* Howell, John R. and Perlmutter, Morris. s.l. : Journal of Heat Transfer, Vol. 12. pp. 547 - 560.
[15] *The Monte Carlo Method in Radiative Heat Transfer.* Howell, John. s.l. : Journal of Heat Transfer, 1997, Vol. 120. pp. 547 - 560.
[16] *Codes for Solar Flux Calculation Dedicated to Central Receiver System Applications: A Comparative Review.* Garcia, Pierre, Ferriere, Alain and Bezian, Jean-Jacques. 3, s.l. : Solar Energy, March 2008, Vol. 82. pp. 189 - 197.
[17] Ho, Cliff. Personal Comminucation via e-mail. *Sandia National Laboratory.* October 2010.
[18] Leary, P. L. and Hankins, J. D. *A User's Guide for MIRVAL.* s.l. : Sandia Laboratories, 1979.
[19] Howell, John R., Siegel, Robert and Menguc, M. Pinar. *Thermal Radiation Heat Transfer.* s.l. : CRC Press, 2010.
[20] *Optical Constant of Silica Glass from Extreme Ultraviolet to Far Infrared at Near Room Temperature.* Pilon, Laurent, Kitamura, Rei and Jonasz, Miroslaw. Los Angeles, CA : CA: Applied Optics, November 2007, Vol. 46.
[21] Duffie, John A. and Beckman, William A. *Solar Engineering of Thermal Processes.* s.l. : Wiley, 2006.
[22] http://heraeus-quarzglas.com/en/home/Home.aspx. *Heraeus Quarzglas - Home of Quartz solutions.* [Online] Heraeus.
[23] Brewster, M. Quinn. *Thermal Radiative Transfer & Properties.* s.l. : Wiley, 1992.

Copyright © 2013 by ASME